Single-layer active-passive Al_2O_3 at the wafer level: optimization study

C.I. van Emmerik, M. Dijkstra, L. Chang, M. de Goede, J. Mu
and Sonia M. Garcia-Blanco

Mesa+ Institute, University of Twente, P.O. Box 217, 7550 AE, Enschede, The Netherlands

Amorphous Al_2O_3 is an attractive platform for integration of active and passive photonic functionalities. We developed an integration procedure to create active regions in a passive layer at the same level on one wafer using reactive co-sputtering of Al_2O_3, with and without shadow mask, and chemical mechanical planarization (CMP). We studied (i) the influence of the deposition height on the uniformity of a passive Al_2O_3 layer and (ii) the influence of the shadow mask on the deposition of active regions. Furthermore we investigate the optimal parameters for planarization.

Introduction

Amorphous Al_2O_3 is an attractive material for integration of active and passive functionalities on a photonic chip. A refractive index of ~1.65 and low propagation losses [1] makes Al_2O_3 a suitable material for devices with a small footprint. The material has the ability to host high concentrations of rare-earth ions with moderate quenching of luminescence [2]. This, in combination with a transparency window ranging from the UV to the mid-IR, makes amorphous Al_2O_3 suitable to dope with various rare-earth ions for on-chip active devices [3].

Amorphous rare-earth doped Al_2O_3 is used in many lasers and amplifiers as gain material [4] in the last few years and is already integrated with other passive photonic platforms like S_3N_4 [5]. Those integration schemes rely on multiple photolithography steps, which introduce losses due to misalignment [6].

We have previously demonstrated the proof of principle of the integration of active, ytterbium doped Al_2O_3 regions in a passive Al_2O_3 surrounding by the luminescence of a ring resonator in the active region [7]. In this paper we show the optimization study including the uniformity of the deposited layer and the chemical mechanical polishing (CMP) parameters.

Deposition of active and passive Al_2O_3 layers

The process flow for the fabrication of active-passive Al_2O_3 layers is shown in figure 1. First ytterbium doped Al_2O_3 regions are deposited through a shadow mask. Those regions are then overgrown by thicker undoped Al_2O_3 to obtain a complete layer. Before patterning, the layer is planarized using CMP. Afterwards the devices can be patterned in a single lithography and etching step. A full description of the process can be found in [7].

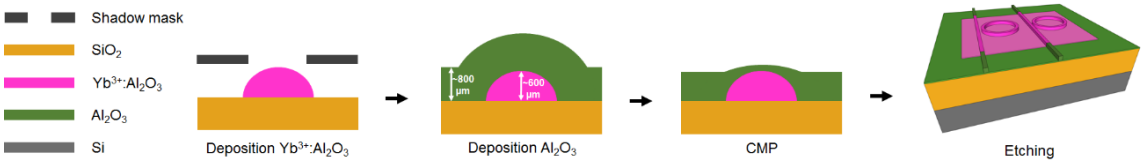

Figure 1: Schematic representation of the fabrication flow of one layer active-passive Al_2O_3.

The active Yb^{3+} doped Al_2O_3 regions are deposited through a shadow mask made out of 200 µm thick molybdenum. The openings with a width of 650 µm and various lengths are made by laser cutting (Rofin MPS). The active regions turned out to be curved with a wider width at the bottom than the width of the shadow mask, as shown in figure 2(a). The areas did not reach a flat plateau at the target height of ~600 nm because the influence of the sidewall of the mask (200 µm) is too big compared to the width of the areas (650 µm).Therefore a new mask was made with minimal opening width of 2 mm, to ensure an uniform top height over at least 650 µm width (figure 2(a) blue line).
The next step in the process is the deposition of an uniform undoped Al_2O_3 layer. The uniformity of the deposited Al_2O_3 layer was studied at different heights between the sputtering target and the wafer (deposition height). The deposition height in the AJA ATC 1500 instrument can be adjusted from 1 to 7 inch in accurate steps of 0.25 inch. In previous studies, a deposition height of 6.75 inch was used. Here we deposited a thin layer of ~50 nm on a silicon wafer at room temperature at 5.00, 6.00 and 6.75 inch. The results are shown in figure 2(b), where the curvatures are normalized by the value at the center of the wafer. The curvature of the wafer changes from convex to concave when the distance between the target and wafer becomes smaller. An additional deposition height of 5.75 inch was tested to see where the inflection point would occur, which happens between 5.75 and 6.00 inch. The change in curvature could be caused by the way the material is sputtered from the target and accelerated to the wafer. A deposition height of 6.00 inch was finally chosen because it has the highest uniformity.
The optical quality of the layer was checked by depositing a layer with the settings described in [7] and checked by prism coupling (Metricon 2010/M) light at a wavelength of 633 nm into the layer.

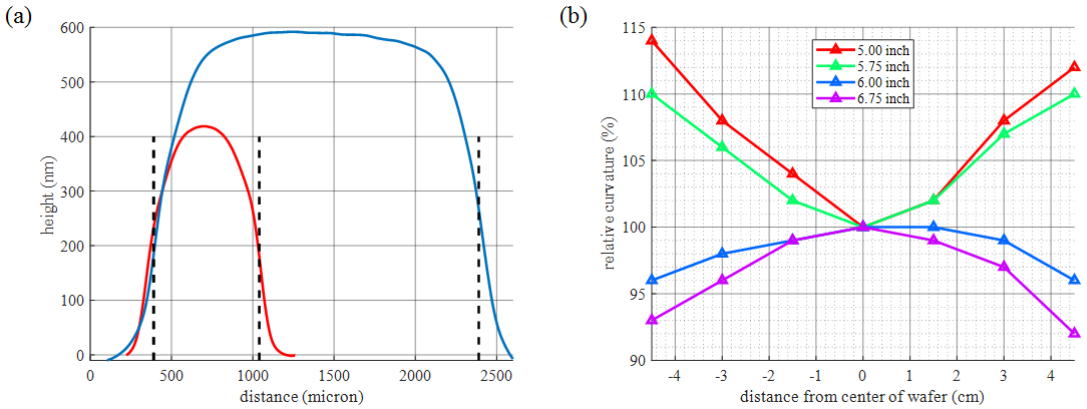

Figure 2: (a) Profile scan of the deposited Yb^{3+}:Al_2O_3 areas for a mask width of 650 µm (red) and 2000 µm (blue), vertical dashed lines represent the position of the sidewalls of the shadow mask. (b) Normalized line layer thickness of Al_2O_3 layer at different deposition heights.

Planarization efficiency

After the double deposition described above, there is an topology on the layer with approximately the same dimensions as the deposited regions (Figure 1). This topology has to be removed before devices can be patterned, which will be done using chemical mechanical planarization (CMP).
For this application, it is very important to achieve a very high planarization efficiency (PE). During the CMP process, material will be removed from the top of the bump regions and from the complete surface of the wafer with different removal rates. The planarization efficiency is given by:

$$PE = \left(1 - \frac{\Delta down}{\Delta up}\right) \cdot 100\% \quad (1)$$

Where, Δup is the material removed at the top of the bumps, Δdown is the material removed at the surface of the wafer at any instant during the planarization process [8]. In a good planarization process, PE should be close to one, which means that the height of the bumps is removed much faster than the surface of the wafer. The step height of the bumps is measured before and after the process with a line scan (Veeco Dektak 8) and the wafer region is measured with ellipsometry (Woollam M-200UI).

The available slurry is Carbot Semi Sperse 25 (SS25), which consist of fumed SiO_2 particles. This slurry has a pH of 12 when diluted 1:2 with DI water. Al_2O_3 or better $Al(OH)_3$ dissolves in alkaline solutions [9], which enhance the chemical removal rate of the material. For our application, we target a more mechanical driven removal and therefore the slurry was adjusted to a pH of 7 by adding 2% HCl solution.

The CMP procedure is done with Mecapol E460 in combination with a DOW-IC1000 grooved SUBA pad. The slurry flow is kept constant at 240 ml/min during the whole procedure. At the start of every run the polishing pad is conditioned with 2 sweeps with a diamond disk to establish the same roughness of the pad. A back pressure of 0.2 bar holds the wafer onto the head. The CMP procedure takes 30 seconds where the rotation speed of the head is 1 rpm less than that of the platen.

For the first experiment, the PE was studied as function of the velocity of the platen. During the process the pressure was set to 0.75 bar. From the results shown in figure 3(a) can be seen that the PE decreases linearly with rotation speed. For the second experiment, the PE was studied as function of the pressure on the wafer. During the process the rotation speed of the platen was set to 50 rpm. Also here the PE decreases linearly with higher pressure on the wafer, as shown in figure 3(b). The data point at 0.5 bar did not follow the trend and no clear explanation could be found to explain this point.

The experiments made at a rotation speed of 50 rpm and a pressure of 0.75 bar are slightly different (fig 3(a) PE = 48% , fig 3(b) PE= 76%). This difference can be caused by the fact that the mechanical properties of both wafers are slightly different. In a multi-user cleanroom it could also be that the condition of the deposition and CMP machines change due to different processes which also influence the process. Therefore the presented results can only be used as guideline.

The PE does not say anything about the removal rate during the process. For an high removal rate of the upper part (~80 nm in 30 sec) a pressure of 0.75 bar with an rotation speed between 30-50 rpm is optimal. While for the final smoothening and high precision removal a low pressure or rotation speeds is beneficial.

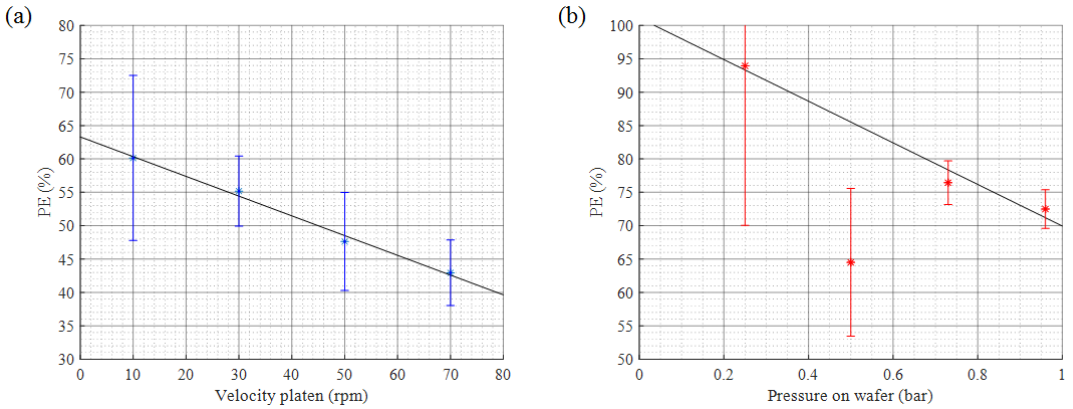

Figure 3: (a) Planarization efficiency as function of the rotation velocity of the platen. (b) Planarization efficiency as function of the pressure on the wafer.

Conclusion

For the integration of active Yb^{3+}:Al_2O_3 areas in a passive Al_2O_3 layer, it is important that the openings in a shadow mask are large enough to obtain a plateau region for the targeted layer thickness. For our application this means that at least 2 mm wide regions are needed to obtain a flat layer for a thickness of roughly 600 nm. Further an optimal deposition height of 6 inch was found for the most uniform layer. The influence of the rotation speed of the platen and the pressure on the wafer on the planarization efficiency have been investigated.

Funding

This project has received funding from the European Research Council (ERC) Horizon 2020 research and innovation programme, grant agreement no. 648978 (RENOS).

References

[1] K. Wörhoff, J. D. B. Bradley, F. Ay, D. Geskus, T. P. Blauwendraat, and M. Pollnau, "Reliable Low-Cost Fabrication of Low-Loss Al_2O_3:Er^{3+} Waveguides With 5.4-dB Optical Gain," *IEEE J. Quantum Electron.*, vol. 45, no. 5, pp. 454–461, May 2009.

[2] S. A. Vázquez-Córdova, M. Dijkstra, E. H. Bernhardi, F. Ay, K. Wörhoff, J. L. Herek, S. M. García-Blanco, and M. Pollnau, "Erbium-doped spiral amplifiers with 20 dB of net gain on silicon," *Opt. Express*, vol. 22, no. 21, p. 25993, Oct. 2014.

[3] T. Ishizaka and Y. Kurokawa, "Optical properties of rare-earth ion (Gd^{3+}, Ho^{3+}, Pr^{3+}, Sm^{3+}, Dy^{3+} and Tm^{3+}) -doped alumina films prepared by the sol–gel method," *J. Lumin.*, vol. 92, no. 1–2, pp. 57–63, Dec. 2000.

[4] G. Singh, P. Purnawirman, J. D. B. Bradley, N. Li, E. S. Magden, M. Moresco, T. N. Adam, G. Leake, D. Coolbaugh, and M. R. Watts, "Resonant pumped erbium-doped waveguide lasers using distributed Bragg reflector cavities.," *Opt. Lett.*, vol. 41, no. 6, pp. 1189–92, 2016.

[5] M. Belt and D. J. Blumenthal, "High Temperature Operation of an Integrated Erbium- Doped DBR Laser on an Ultra-Low-Loss Si_3N_4 Platform," vol. 79, no. 3, pp. 8–10, 2015.

[6] J. Mu, M. Dijkstra, Y.-S. Yong, F. B. Segerink, K. Wörhoff, M. Hoekman, A. Leinse, and S. M. García-Blanco, "Low-loss, broadband and high fabrication tolerant vertically tapered optical couplers for monolithic integration of Si_3N_4 and polymer waveguides," *Opt. Lett.*, vol. 42, no. 19, p. 3812, Oct. 2017.

[7] C. I. van Emmerik, M. Dijkstra, M. de Goede, L. Chang, J. Mu, and S. M. Garcia-Blanco, "Single-layer active-passive Al_2O_3 photonic integration platform," *Opt. Mater. Express*, vol. 8, no. 10, p. 3049, Oct. 2018.

[8] Y. Hong, V. K. Devarapalli, D. Roy, and S. V. Babu, "Synergistic Roles of Dodecyl Sulfate and Benzotriazole in Enhancing the Efficiency of CMP of Copper," *J. Electrochem. Soc.*, vol. 154, no. 6, p. H444, Jun. 2007.

[9] K. Wefers and C. Misra, *Oxides and Hydroxides of Aluminum*, vol. 19. 1987.